6

GPR Environmental-Based Landmine Automatic Detection

Zakarya Zyada, Yasuhiro Kawai, Shinsuke Sato, Takayuki Matsuno, Yasuhisa Hasegawa and Toshio Fukuda
Nagoya University
Japan

1. Introduction

According to the United Nations, as of the year 2000 there were 70 million landmines planted in a third of the world's nations affecting global causality rate of up to 20,000/year, (Anderson, 2002). That is why landmine detection has attracted much attention by many research teams around the world during the last two decades; among them is our research team in Nagoya University. Anti-personnel (AP) mine ranges from 5 to 15 cm in size; they can be metal, plastic, or wood. AP mines are normally buried at shallow depth; detonated by very low pressure, and designated to kill or maim people. PMN2, Type72 and PMN are examples, Fig. 1. In real world clearance activities, AP mine suspect areas are divided into 1 m grid squares, and each square meter is probed with a bayonet or plastic rod. Probing is done at an oblique angle to the ground so that the rod will encounter the side of a land mine and not trip the fuse. No need to say, this work is very dangerous and proceeds very slow, (Siegel, 2002). The need for a safer and more fast humanitarian demining action by replacing a manual sensing task by vehicle sensing task have motivated our research team to introduce a low-ground-pressure tires detection vehicle, (Hasegawa et al, 2004-A). The unmanned vehicle that can move in mine field without detonating a group of AP mines will be presented in this chapter.

One of the big challenges in demining process is detection. If a mine is detected, deminers can explode, mark or move it to a pit for later detonation or defusing. Conventional mine detection, by a metal detector, is often difficult for two reasons. First, mines are increasingly being made of plastics, minimizing the more easily detectable metal components. Second, mined areas are often equipped with metal scraps creating a high false alarm rate. Because of the difficulty encountered in detecting the tiny amounts of metal in a plastic landmine with a metal detector, technology development has been extended to other sensors. Ground penetrating radar (GPR) used for about 70 years for a variety of geophysical subsurface imaging applications including utility mapping and hazardous waste container has been actively applied to the problem of land mine detection for nearly the last two decades of research. It provides sensing objects underground based on dielectric properties. It senses the reflected electromagnetic wave by a buried object. It is expected that GPR be a good alternative sensor and/or an important support sensor when fused with a metal detector for

Source: Humanitarian Demining: Innovative Solutions and the Challenges of Technology, Book edited by: Maki K. Habib, ISBN 978-3-902613-11-0, pp. 392, February 2008, I-Tech Education and Publishing, Vienna, Austria

landmine detection. However, one major source of error in GPR data is the reflection from the surface of the ground, (Daniels, 2004). The problem becomes much more difficult for an undulating ground-surface. As a general objective of signal processing as applied to GPR is to present an image that can be easily interpreted by the operator, it is important to adapt the signal processing technique for an undulating surface scanning. In this chapter, ground-surface-adaptive scanning and signal processing for ground-surface-adaptive scanning, (Hasegawa et al, 2004-B), applying a vector GPR, (Fukuda et al, 2006; Fukuda et al, 2007), will be presented.

A metal detector is one of the most major sensors applied for current humanitarian demining. It is simple and cost effective. It is also reliable to find an anti-personal mine (APM) in a shallow subsurface. However it suffers from the high false alarm rate, (about 99.95%), as it senses all metal objects including metal fragments in the field other than land mines. On the other hand, ground penetrating radar provides, (after processing), images for objects underground based on dielectric properties. However it senses a land mine object as well as any other object as it senses dielectric discontinuities in metallic and/or non-metallic objects. Fusion of GPR with MD is expected to minimize the false alarm rate significantly. In this chapter, fusion of both MD and GPR for APM detection in a shallow subsurface is presented. A "feature in-decision out" fuzzy sensor fusion algorithm for GPR and MD is introduced, (Zyada et al, 2006-A). The inputs to the fuzzy fusion system are features extracted from both GPR and MD measurements. The output from the fuzzy fusion system is a decision if there is a land mine and at what depth it would be. Fuzzy fusion rules are extracted from training data through a fuzzy learning algorithm. Experimental test results are presented to demonstrate the validity of the proposed fuzzy fusion algorithm and hence its influence in minimizing the false alarm rate for mine detection, (Zyada et al, 2007).

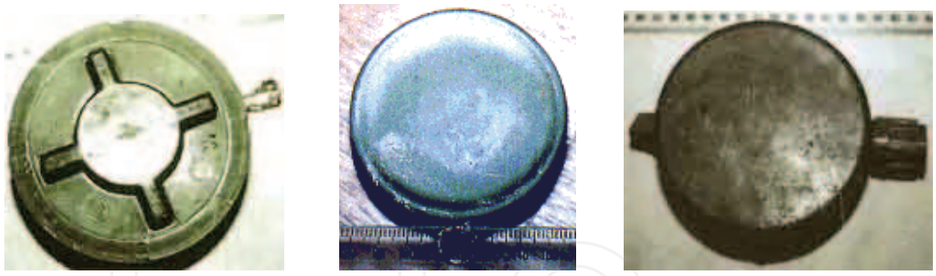

(a) (b) (c)

Fig. 1. Anti-personnel landmine samples: (a) PMN2; (b) Type72; (c) PMN.

This chapter is organized as follows: Section 2 introduces a low-pressure-tire vehicle capable of moving inside a mine field without detonating a group of antipersonnel landmines. This vehicle is applied as a sensor manipulator. Section 3 presents the enhancement of landmine images through signal processing of a scanned undulating surface applying a vector frequency modulated continuous wave (FMCW) GPR. Section 4 presents the fuzzy fusion algorithm of GPR with MD for antipersonnel landmine automatic detection. Learning fuzzy fusion rules as well as experimental evaluation of the learnt fusion rule base, is also presented. Section 5 presents conclusions and projected work.

¶

2. Low-pressure-tire Vehicle

General demining method is exploring with a probe or with a metal detector by an operator, (Shimoi, 2002; Genève international centre, 2004). However, it is not few cases that the workers suffer damage during the demining process. Then, robot-based demining in place of human-based demining has been investigated by many researchers. Most of them move in the minefield evading the landmine (Nonami, 2002; Kato, 2001). Complex mechanism and big cost is needed for building an evading robot. In contrast, a simple and low cost system is needed in affected areas. In this section, a mine detection vehicle which can enter a minefield and detect landmines directly without detonating landmines is introduced.

2.1 In-minefield Vehicle

By this sub-title, it is meant that the vehicle can enter a mine field without detonating its landmines. In order to enter a mine field, this system uses low landing pressure tires. Stiffness of these tires is much lower than that of ordinal ones, so that the area contacting the ground is very large and the load on the tire is distributed over the area. Access Vehicle is made of a commercial available leisure cart. This vehicle equips 4 low landing pressure tires and electric motors for driving. Figure 2 shows its appearance. Access vehicle carries battery as power supply in order to work without any cable. It also carries 2 laptop PCs for the purpose of motor and GPR control. These PCs are used to receive commands from operator via wireless LAN (IEEE802.11b) . On the other hand, Operator's Instrument consists of a laptop PC and a laser total station for position measurement. Operator's Instrument communicates with access vehicle using PC, and acquires position of the Access Vehicle by the total station. Data from sensor are stored to a PC on Access Vehicle temporally, transmitted to Operator's Instrument timely, and recorded with position of vehicle to Information Management System, (Hasegawa et al, 2004-B). Utilizing a commercial available cart as a frame shortens the time period of development and reduces cost. Access vehicle's total weight including sensor and sensor manipulator is about 90 kgs, so load on each tire is about 22.5 kg. Low landing pressure tires for this vehicle are made by Roleez Wheels, Inc. in U.S.A.

2.2 Subsurface Forces

To check the validity of the access vehicle for entering a minefield without detonating landmines, a group of experiments have been executed. A force sensor is buried under the ground surface for a range of 0~20 cm. Subsurface forces as well as the detonating pressure force for a group of anti-personal landmines are shown in Fig. 3. These values are average stress, load divided by the area of force sensor. Maximum pressure amounts to 0.063 [kg/cm2]. This result means that landing pressure of this vehicle is less than that of small landmines such as Type-72 (0.19 [kgf/cm2]) and PMN2 (0.26 [kgf/cm2]), but almost the same as PMN (0.064 [kgf/cm2]), and bigger than PMA-1 (0.031 [kgf/cm2]). Considering these landmines' small ignition force (3kgf, 5kgf), PMN or PMA-1 anti personnel landmine have large areas to receive force so it is very hard to apply low landing pressure vehicle to a minefield which contains these kinds of landmines. Clearly, even though this vehicle has a contact pressure smaller than many anti-personnel land mines ignition pressure, it cannot enter the minefield which contains some types such as PMA-1 and PMN. The vehicle is

currently under developing its tires to distribute force to larger area. Furthermore equipping two tires on one axle would raise its safety coefficient.

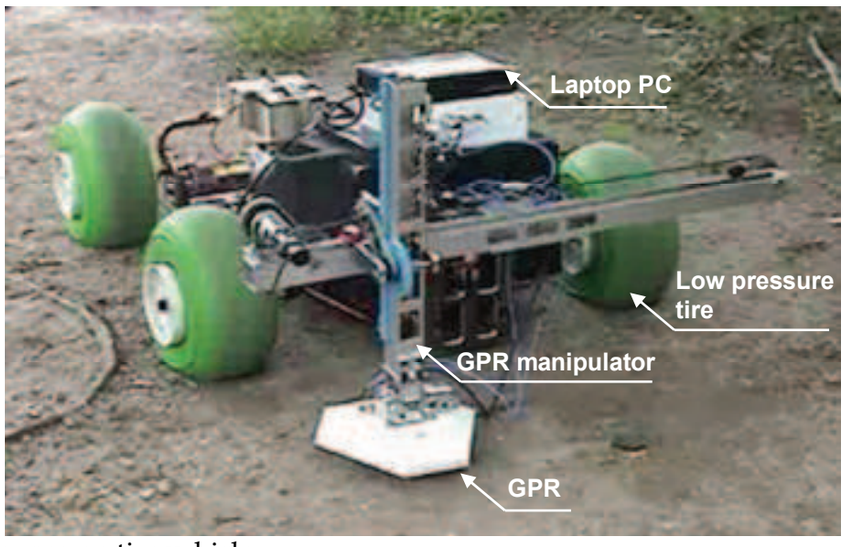

Fig. 2. Low-pressure-tire vehicle

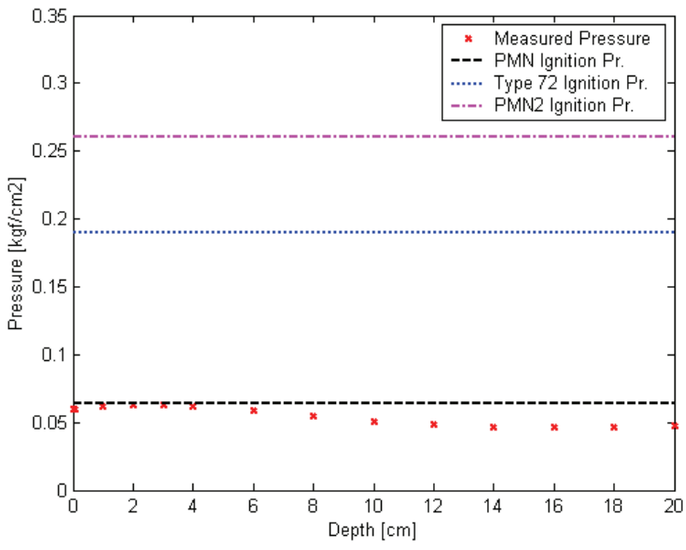

Fig. 3. Sub-surface pressure and ignition pressure for a group of anti-personnel mines

3. Environmental-adaptive GPR Manipulation and Signal Processing

Ground Penetrating Radar (GPR) is expected to be a good alternative sensor or support device of metal detector for humanitarian demining. GPR system measures the response time of reflected electromagnetic wave caused by buried objects, and it is originally used for archeological digging, detection of underground pipe and detection of lack in reinforced concrete. Though GPR performance is expected to be high for land-mine detection, there are

many problems encountered in the sening process. Among them, (1) decrement of an electromagnetic wave becomes large, and performance turns worse by a water content of the soil; (2) reliability of detection result deteriorates when operation is conducted with non-homogeneous soil; (3) if there are irregularities or a slant in a ground surface, they are projected onto an image of the underground. As a result, it becomes difficult to distinguish a shallow underground object. For the first problem, it can be overcomed by choosing the electromagnetic wave frequency that is hard to be absorbed by soil water content; fusion with a metal detector is effective for solving the second problem. However, because the last problem cannot be solved by fusion with metal detector beyond the maximum depth at which a metal detector can sense, it cannot be overcomed. Trying to solve the third problem, the enhancement of mine detection, applying a vector type ground penetrating radar (Kimura et al., 1992 ; Murasawa et al.., 1992), that is adaptively scanning the ground surface, (Fukuda et al, 2003; Hasegawa et al, 2004-B), is presented.
In this section, an environmental-adaptive GPR manipulation and signal processing is presented. First, the applied ground penetrating radar sensor and concept of geography adaptive scanning are introduced. Then, image enhancement based on signal processing for geography adaptive scanning applying FMCW GPR and imaging results are introduced.

3.1 Ground Penetrating Radar (GPR) Sensor

A three-element vector stepped-frequency ground penetrating radar (GPR) system, Fig. 4, developed by Mitsui Engineering and Ship Building Company, (Japan), is applied in this study. It is an ultra-wide bandwidth vector type GPR. Its frequency bandwidth is 7.8125 MHz – 2.0 GHz. Its frequency is changed in 256 steps.

Fig. 4. Ground Penetrating Radar (GPR) system

3.2 Concept of Geography Adaptive Scanning

Ground surface reflects most power of an electromagnetic wave transmitted by GPR antenna because of the big difference of permittivity of the atmospheric layer with respect to ground surface. It is important to eliminate the ground surface effect. Elimination of ground surface effect is done by letting the antenna trace the ground configuration. The concept of geography adaptive scanning is shown in Fig. 5. The ground configuration is measured by a laser range finder, as will be presented later in this section.

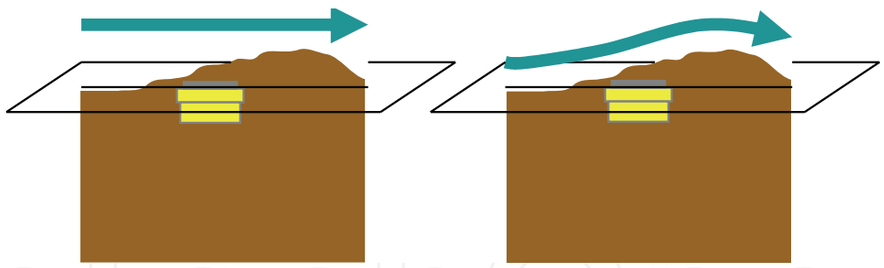

(a) (b)

Fig. 5. Scanning methods: (a) Flat scanning; (b) Geometric adaptive scanning

3.3 GPR Images Enhancement for Geography Adaptive Scanning

It is known that frequency modulated continuous wave FMCW radar systems have been used in preference to AM systems where the targets of interest are shallow and frequencies above 1 MHz can be used, (Daniels, 2004). Since a GPR response signal is reflection intensity versus time, image reconstruction is required for easier extraction of mine suspects, for both easier interpretation and automatic detection, (Yilmaz, 1987). For this purpose, many signal processing methods have been proposed and applied to GPR imaging, but most of them have only considered a measuring system which maneuvers an antenna flatly regardless of geography. In this section, the signal processing technique applicable to geography adaptive antenna applying a vector GPR is summarized. GPR signal processing includes two main steps to obtain image spatial distribution. These steps are: suppression of reflection from ground surface and and migration.

3.3.1 Suppression of reflection from ground surface

A local average subtraction is applied for better clutter suppression. The local average subtracted signal $\phi_i'(t)$ is given by $\phi_i'(t) = \phi_i(t) - \overline{\phi}_i(t)$ where $\phi_i(t)$ is the raw data and $\overline{\phi}_i(t)$ is local average signal at sensing point i; $\overline{\phi}_i(t) = \frac{1}{n_i}\sum_{k\in K_i}\phi_k(t)$ where K_i is a set of sensing points in the neighborhood of sensing point i and n_i is the number of members of K_i.

A time series signal is obtained through Inverse Fast Fourier Transformation. Given the frequency domain signal $\psi_v\left(\mathrm{x},\mathrm{y},\mathrm{z},{}^{\mathrm{B}}_{\mathrm{S}}\mathrm{R},\mathrm{m},\mathrm{f}\right)$ measured by the wide range stepped frequency radar, we can get the time domain signal through Inverse Fourier Transform

$$\begin{aligned}\phi_v\left(x,y,z,{}^{B}_{S}R,m,t\right) &= \mathrm{IFT}_{\mathrm{f}}\left\{\psi_v\left(\mathrm{x},\mathrm{y},\mathrm{z},{}^{\mathrm{B}}_{\mathrm{S}}\mathrm{R},\mathrm{m},\mathrm{f}\right)\right\} \\ &= \frac{1}{\sqrt{2\pi}}\int_{-\infty}^{\infty}\psi_v\left(\mathrm{x},\mathrm{y},\mathrm{z},{}^{\mathrm{B}}_{\mathrm{S}}\mathrm{R},\mathrm{m},\mathrm{f}\right)e^{j2\pi ft}df\end{aligned} \tag{1}$$

where $\phi_v\left(x,y,z,{}_S^B R,m,t\right)$ is the reflected wave; $[x,y,z]^T$ is the centre position of antenna; ${}_S^B R$ is the rotation matrix of center of sensor head; m is polarization mode; t is the time between emitting and receiving; z is the ground surface function, $z=z_g(x,y)$, (obtained through measurements); x,y are its arguments.

A 3-D GPR spatial signal is reconstructed from the time signal. Kirchhoff migration is adopted to reconstruct the spatial distribution of subsurface reflectivity from a set of time series signals acquired on the ground surface by three-element vector radar.

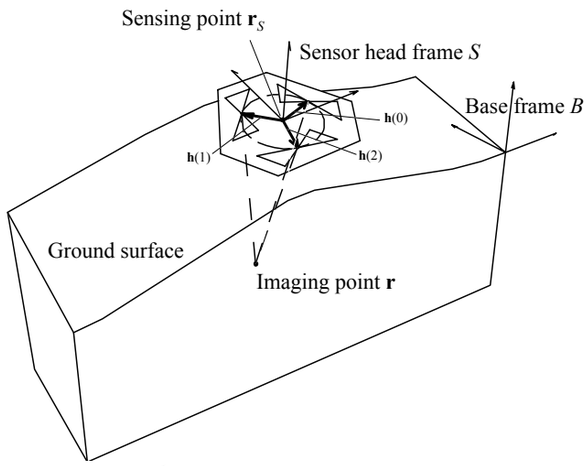

Fig. 6. Alignment of an antenna and imaging point

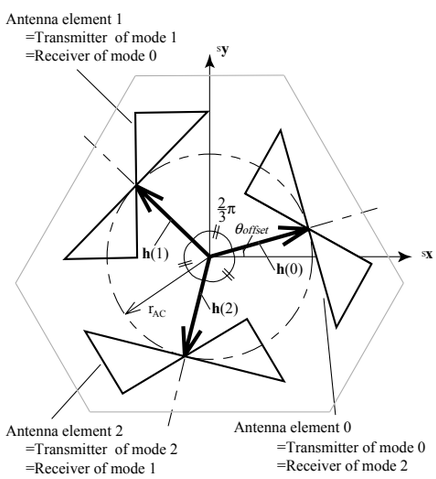

Fig. 7. Layout of antenna elements

3.3.2 Migration

Migration is a method to reconstruct the spatial distribution of subsurface reflectivity from a set of time-series signals acquired on the ground surface. This method has been studied in seismology (Yilmaz, 1987), and applied to GPR in some cases, (Feng and Sato, 2004).

Several kinds of migration are known, such as diffraction stacking, Kirchhoff migration, f-k migration, FD migration, and reverse time migration. Kirchhoff migration has been chosen here because it is easy to be implemented and to give physical meanings, (Schneider, 1978). The migration process will be summarized here. Figure 6 shows coordinate system of GPR. Here, position of focused point under ground is indicated as $P=[x,y,z]^T$, and center position of three antennas at measurement point is indicated as $P_S=[x_S,y_S,z_g(x_S,y_S)]^T$. Then, reflection rate $\sigma(x,y,z)$ is expressed as:

$$\sigma(x,y,z)=\sum_{m=0}^{m=2}\int\int_{-\infty}^{\infty}\frac{\cos\theta}{r^2}\phi_v(x_S,y_S,m,t_P)dx_S dy_S \tag{2}$$

where, $r=\|P_S-P\|$; $\cos\theta=n_g(x_S,y_S)\cdot(P_S-P)/r$; $n_g(x_S,y_S)$ is the unit vector of ground surface; t_P is the traveling time of electromagnetic wave and expressed as $t_P=(\|P_T-P\|+\|P_R-P\|)/v$; v is the propagation velocity of electromagnetic wave; $P_T=P_T+{}^B_S R(P_S)\,{}^S h(i_T(m))$; $P_R=P_R+{}^B_S R(P_S)\,{}^S h(i_R(m))$; $i_R(m)$ is index of receiver antenna; $i_T(m)$ is index of transmitting antenna; m is the mode as shown in Fig. 7. ${}^B_S R(P_S)$ is rotation matrix of center of antennas frame $\{S\}$ with respect to the base frame. $\{B\}$; ${}^S h(i_R(m))$: position of i antennas element viewed from $\{S\}$.

$${}^S h(i_R(m))=\begin{bmatrix} r_{AC}\cos(\frac{2\pi}{3}i+\theta_{offset}) \\ r_{AC}\sin(\frac{2\pi}{3}i+\theta_{offset}) \\ 0 \end{bmatrix} \tag{3}$$

3.4 Imaging Results

The validity of signal processing for geography adaptive scanning was investigated through experiments. A buried object as applied for this evaluation is a plastic case of the shape of Type 72 landmine, Fig. 8. Dry sand with 3% water content inside a tank with its surface is formed with inclined plane. Its surface data measured by a laser range finder is shown in Fig. 9. The ground surface is flatly and adaptively scanned as shown in Fig. 5. The results of flat and geography adaptive scans after signal processing are shown in Fig. 10. As shown in Fig. 10(a), effect of ground surface remains and the shape of landmine deforms according to it. On the other hand, when scanned adaptively to ground surface, disturbance according to ground surface hardly remained and the target-clutter ratio enhances, especially for shallow buried object, Fig. 10(b). The effect of polar modes is shown in Fig. 12 and the

effectiveness of the synthesized modes for 3-antenna radar is shown Fig. 12d. Appearance of adaptive scanning experiment is shown in Fig. 11.

Fig. 8. Buried object: plastic case of a landmine shape

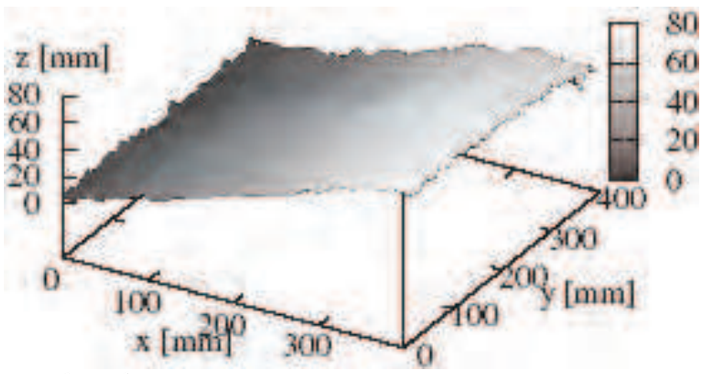

Fig. 9. Shape of ground surface

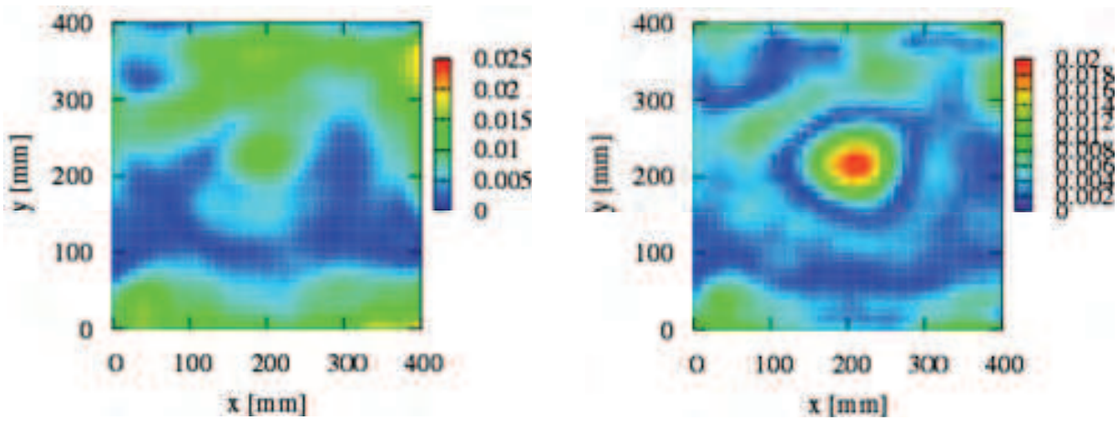

(a) (b)

Fig. 10. C-scan results applying: (a)Flat scanning; (b)Geometric adaptive scanning

(a) (b) (c)

Fig. 11. Appearance of adaptive scanning experiment

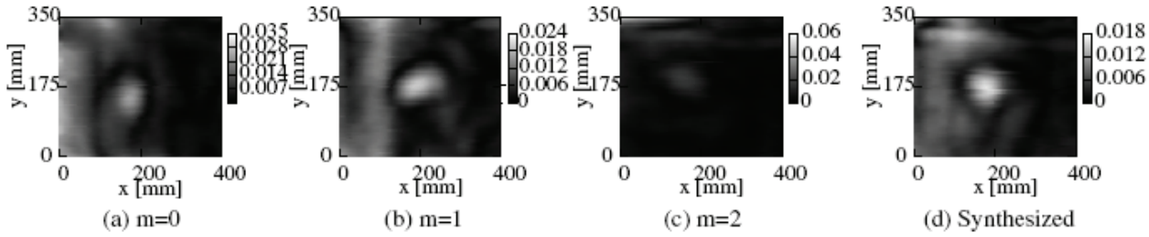

(a) m=0 (b) m=1 (c) m=2 (d) Synthesized

Fig. 12. C-scan views processed with various polar modes

4. GPR-MD Fuzzy Fusion

In this section, an automatic sensor-fusion based detection algorithm of an anti-personnel land mine is presented. A "feature in-decision out" fuzzy sensor fusion algorithm for a ground penetrating radar, (GPR), and a metal detector, (MD), for anti-personnel landmine detection is introduced. The inputs to the fuzzy fusion system are features extracted from both GPR and MD measurements. The output from the fuzzy fusion system is a decision if there is a land mine and at what depth it would be. Fuzzy fusion rules are extracted from training data through a fuzzy learning algorithm. Experimental test results are presented to demonstrate the validity of the proposed fuzzy fusion algorithm and hence its influence in minimizing the false alarm rate for humanitarian demining.

4.1 Experimental System

A six-degree of freedom serial manipulator of type PA10-7C, manufactured by Mitsubishi Heavy Industries, Japan, is applied as a sensor manipulator for GPR-MD sensor fusion. Manipulator based scanning facilitates a regular step scanning better than a manual based scanning, which leads to better signal processing results. Another advantage is the safety achieved by automatic scanning as an operator can do his task from a remote place. PA10 manipulator holding a metal detector is shown in Fig. 13. Avoiding the manipulator singularity points, it was possible to design the same path for both GPR and MD sensors. The test field is a tank full of dry and homogeneous river sand, as shown in Fig. 13. Its water content is 4.0 %, (relative permittivity of about 3.29). EM wave absorber covers all the sidewalls and the bottom of the tank to suppress the tank walls reflection during GPR measurements. A dummy land mine of type PMN2 is the applied one for demonstrating the methodology of this study, Fig. 14. It has the same dielectric constant and the same

metal content as the real one. Its diameter and height is 122 and 54 mm, respectively. The field is relatively flat and both the GPR antenna and MD sensing head scanned in a path parallel to the surface with a gap between the sensor head and the ground of 10 mm. During the experiments, the scanning area is 400x500 mm². The manipulator movement is in 20 mm steps in both Y-Z directions comprising a grid of 21x26 measurement points by both GPR and MD. The scanning path is as shown in Fig. 15.

Fig. 13. Metal detector manipulation

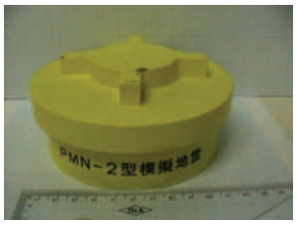

Fig. 14. Dummy PMN2 landmine

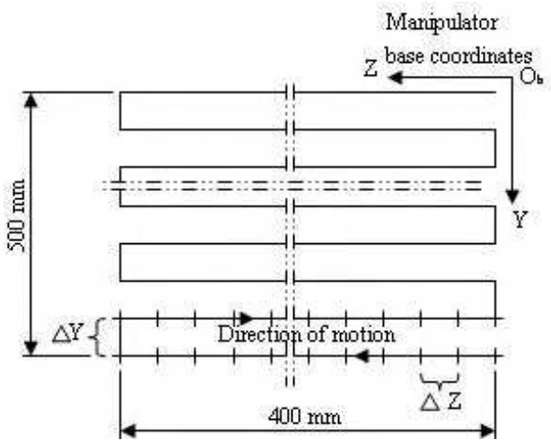

Fig. 15. Scanning path

4.2 Features Extraction

The inputs to fusion algorithm are GPR and MD features while the output is a decision if there is a landmine or not and at what depth it would be. In this subsection, extraction of GPR as well as MD features from the processed data is presented.

4.2.1 GPR Features Extraction

The migrated GPR data, (section 3), gives 3-D reconstructed image, from which horizontal slice image (C-scan), can be extracted. A horizontal slice of reconstructed signal amplitude for a buried PMN2 dummy land mine at a depth of 20 mm is shown in Fig. 16. We use the maximum amplitude from all the different horizontal slices as a feature of GPR measurements. The amplitude as well as position is extracted from the 3-D reconstructed image. It should be noted that A-scan, Fig. 17, for a buried object will have peaks at a depth different from that for a pure ground. As shown in Fig. 17, the reflection intensity of a dummy landmine has two peaks near the surface and at another depth underground, (about 7.0 cm), while that for a pure mine field, (without a landmine), has only one peak at the surface. A peak of reflection intensity underground is an indication of a buried object.

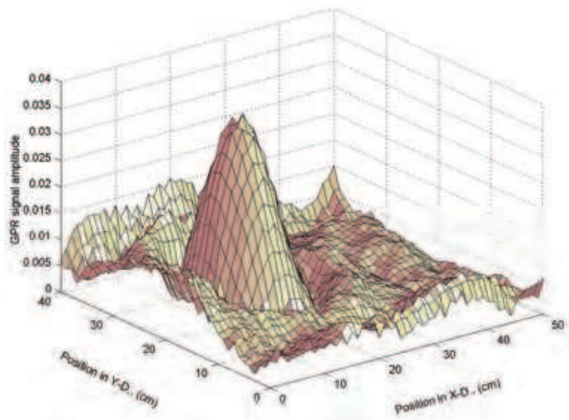

Fig. 16. C-scan of the reconstructed signal amplitude of a dummy PMN2 landmine, (buried at depth 2.0 cm)

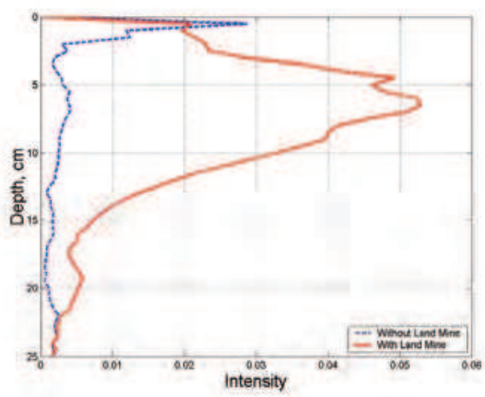

Fig. 17. A-scan of the mine field with and without a landmine

4.2.2 MD Features Extraction

A dual frequency metal detector of type MINEX 2FD 4.500, Fig. 13, manufactured by Forster, (Germany), is applied. The operating principle is based on continuous wave technique, comprising a transmitter coil and two symmetrical receiver coils in a gradient arrangement. The transmitter coil sends one signal continuously at two frequencies. As a result of the induction effect in a conducting object and its return effect on the coil system, the coil impedance changes. This change is evaluated and returned in the form of an acoustic signal. In the current measurement system, the output signal is acquired through a direct wiring interface.

The captured MD time-domain signal is transformed into frequency domain then the peak around the working frequency is captured. For a scanned surface, the output signal is like that shown in Fig. 18. The object position is exactly at the position of changing the sign of amplitudes from positive to negative. We reform this signal to the cumulative sum in X-D, Fig. 19, so as to make it easier in deciding the position of scanned object which is directly at the peak cumulative sum. We take this cumulative sum as an MD feature, (Zyada et al, 2006-A). Cumulative sum, CS_i at point i, is defined as:

$$CS_i = \sum_{y=1}^{y=i} I_{x,y}\Big|_{x=1,\ldots,x_{\max}} \tag{4}$$

It is the summation of the intensity, $I_{x,y}$ from the initial point $(y=1)$ to the current point $(y=i)$ in y direction. That is to be repeated for all values of x. The cumulative sum of the measured signal according to the definition of equation (2) is shown in Fig. 19. The peak amplitude in Fig. 19 as well as its position can be easily extracted. This maximum amplitude is applied as MD-feature of a landmine.

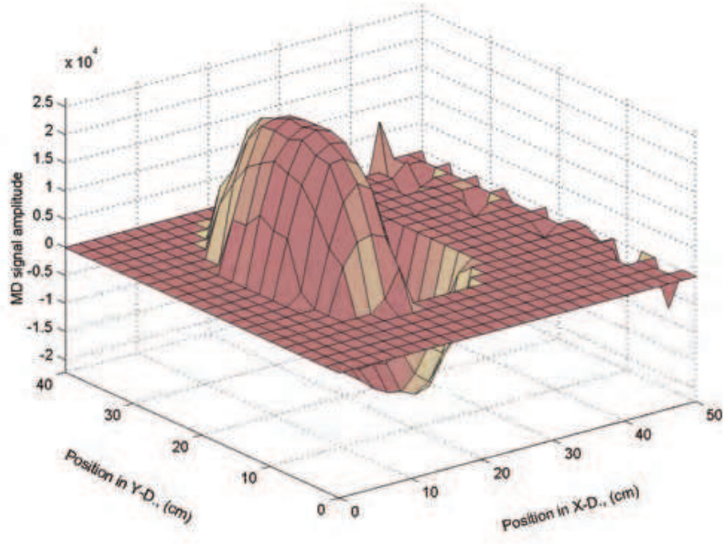

Fig. 18. Metal detector signal amplitude

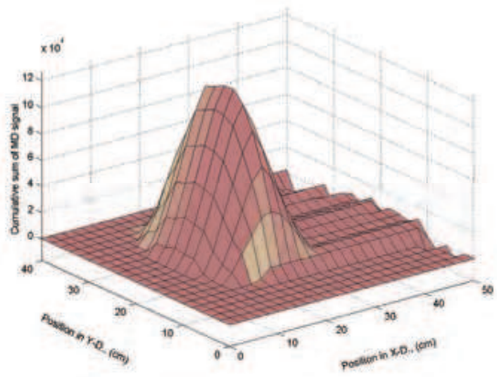

Fig. 19. Cumulative sum of metal detector signal amplitude

4.3 Fuzzy Fusion Rules Learning

We use a fuzzy rule base for fusion of both GPR and MD sensors for humanitarian landmine detection. The learning algorithm applies Wang-Mendel method, [10], for fuzzy rule learning from experimental data.

4.3.1 Learning Fuzzy Rules from Experimental Data

The chosen algorithm for our study, to learn rules from experimental data, is a simplified fuzzy algorithm. It presents three characteristics that make it a good choice in view of our objectives: simplicity, simple one-pass to extract the rules, and flexibility with fast computational time to operate in a demining system. Also, it is possible to collect the learnt rules from numerical data as well as heuristic rules in the same frame of work which may be needed in future development of the current work. This learning algorithm is developed and applied to different applications, (Zyada et al, 2002; Branco and Dente, (1998; 2000-A; 2000-B)).

Fuzzy rules are first learnt from examples then the number of associated membership functions for every variable is optimized for the all learnt rules. The best group of rules expressing data is then selected based on the overall average rules truth degree. In the following, we describe the main steps and a simple example to illustrate the method of extracting fuzzy rule base with two inputs and one output:

Step 1: Choose the Variables and Divide the Input and Output Spaces into Fuzzy Regions: Choose the variables that better characterize the system. The input variables and the output will compose, respectively, the condition and the conclusion of the rule parts. Assume that the domain intervals of variables (x_1, x_2) and y are $[x_1^-, x_1^+]$, $[x_2^-, x_2^+]$ and $[y^-, y^+]$, respectively, where "domain interval" of a variable means that most probably this variable will lie in this interval. Divide each domain interval into an odd number of regions. This number of regions may be different from one variable to another. Assign each region a fuzzy membership function. Use symmetric triangular membership functions whose one of its vertices lies at the center of the region with a membership value of unity and the other two vertices lie at the centers of the two neighboring regions with membership values of zeros as shown in Fig. 20. Other shapes of membership functions are possible. However

authors of the current work applied the stated and examined triangular membership functions proposed by Wang-Mendel, (Wang and Mendel, 1992).

Step 2: Generating Fuzzy Rules from Numerical Data:

From the training set, take the kith numerical data pair

$$(x_1^{(k)}, x_2^{(k)}) \rightarrow y^{(k)} \tag{5}$$

For each input value, $(x_1^{(k)}, x_2^{(k)})$, and corresponding output one, $y^{(k)}$, calculate their respective membership grades in the attributed fuzzy sets. Hence it is constructed for each variable a raw vector denoted by $\vec{m}(x_1^{(k)}), \vec{m}(x_2^{(k)})$ for the inputs and $\vec{m}(y^{(k)})$ for the output, with a number of elements equal to the fuzzy sets attributed in step 1.

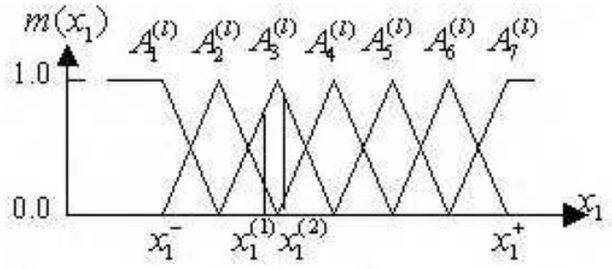

(a)

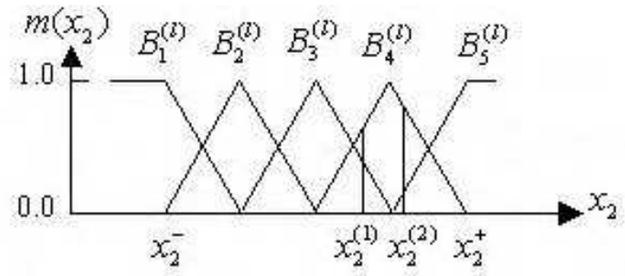

(b)

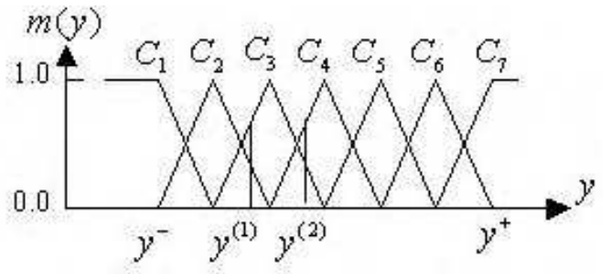

(c)

Fig. 20. Divisions of the input and output spaces into fuzzy regions and the corresponding membership functions, (a) $m(x_1)$, (b) $m(x_2)$, (c) $m(y)$

Choose for each variable their highest membership degree from the grades in the respective vectors, $\vec{m}(x_1^{(k)}), \vec{m}(x_2^{(k)})$ and $\vec{m}(y^{(k)})$. The selected grades are $[\vec{m}(x_1^{(k)})]_{\max}$,

$[\vec{m}(x_2^{(k)})]_{\max}$ and $[\vec{m}(y^{(k)})]_{\max}$. Now, a rule from the kith training pair is obtained. The fuzzy sets attributed for the condition and conclusion parts of this rule are, respectively, the sets A_j, B_j and C_j in which the inputs $(x_1^{(k)}, x_2^{(k)})$ and the output $y^{(k)}$ had maximal membership grades.

Step 3: Assign a Truth Degree to Each Rule:

A truth degree is assigned to each extracted rule as indicated in the following equation. The degree is defined as the product of the highest membership degree of each vector calculated in step 2.

$$\mu(R(k)) = [\vec{m}(x_1^{(k)})]_{\max} \cdot [\vec{m}(x_2^{(k)})]_{\max} \cdot [\vec{m}(y^{(k)})]_{\max}. \tag{6}$$

When two rules have the same fuzzy set in the IF part but a different fuzzy set in THEN part, the rules are called to be in conflict. To resolve this problem, it is accepted only that rule with highest truth degree. At last for this step, if it is not the end of the training data set, the algorithm goes again to the beginning of step 2 to pick up the next data pair.

For completeness, we introduce here an example describing how the learning algorithm in the above three steps operates. We consider for this example a simple case of a system with two input variables (x_1, x_2) and one output variable (y). The variables are partitioned by a number of symmetric triangular membership functions as shown in Fig. 20. Seven fuzzy sets were associated with variable x_1, five fuzzy sets to x_2 and seven fuzzy sets to y.

Suppose a first data pair $(x_1^{(1)}, x_2^{(1)}) \rightarrow y^{(1)}$ collected from the system, which is indicated in Fig. 9. For each input value, compute its membership degree in fuzzy sets A_j or B_j associated to its variable, and do the same for the output variable in its C_j. This procedure results in the following three vectors:

$$\begin{aligned}
\vec{m}_1(x_1^{(1)}) &= [A_1 \;\; A_2 \;\; A_3 \;\; A_4 \;\; A_5 \;\; A_6 \;\; A_7], \\
&= [0.0 \;\; 0.2 \;\; 0.8 \;\; 0.0 \;\; 0.0 \;\; 0.0 \;\; 0.0] \\
\vec{m}_2(x_2^{(1)}) &= [B_1 \;\; B_2 \;\; B_3 \;\; B_4 \;\; B_5], \\
&= [0.0 \;\; 0.0 \;\; 0.4 \;\; 0.6 \;\; 0.0] \\
\vec{m}(y^{(1)}) &= [C_1 \;\; C_2 \;\; C_3 \;\; C_4 \;\; C_5 \;\; C_6 \;\; C_7], \\
&= [0.0 \;\; 0.4 \;\; 0.6 \;\; 0.0 \;\; 0.0 \;\; 0.0 \;\; 0.0]
\end{aligned} \tag{7}$$

Next, choose in each vector of the above three vectors, the fuzzy set with maximum membership degree, resulting in

$$[\vec{m}_1(x_1^{(1)})]_{\max} = \max\{\vec{m}_1(x_1^{(1)})\} \to 0.8 \to A_3,$$
$$[\vec{m}_2(x_2^{(1)})]_{\max} = \max\{\vec{m}_2(x_2^{(1)})\} \to 0.6 \to B_4,$$
$$[\vec{m}(y^{(1)})]_{\max} = \max\{\vec{m}(y^{(1)})\} \to 0.6 \to C_3.$$

From this procedure, the first rule, from the first data pair, (k=1) is extracted, being

$$R_l(1): \text{ IF } (x_1 \text{ is } A_3 \text{ and } x_2 \text{ is } B_4) \text{ THEN } y \text{ is } C_3 \tag{8}$$

A truth degree is attributed to this rule, which is computed by multiplying the membership degrees. That is

$$\mu(R_l(1)) = (0.8)(0.6)(0.6) = 0.288. \tag{9}$$

Suppose now a second data pair $(x_1^{(2)}, x_2^{(2)}) \to y^{(2)}$, indicated in Fig. 9 too, is to be acquired. If we calculate their vectors and their respective maximum membership degrees, the new data pair has the same input fuzzy sets as the rule extracted from the first data pair, although producing an output fuzzy set different from that extracted from the first data pair. In this case we choose the one with maximal degree.

$$\begin{aligned} \vec{m}_1(x_1^{(2)}) &= [A_1 \ A_2 \ A_3 \ A_4 \ A_5 \ A_6 \ A_7], \\ &= [0 \ 0 \ 0.85 \ 0.15 \ 0 \ 0 \ 0] \\ \vec{m}(y^{(2)}) &= [C_1 \ C_2 \ C_3 \ C_4 \ C_5 \ C_6 \ C_7], \\ &= [0 \ 0 \ 0.4 \ 0.6 \ 0 \ 0 \ 0] \end{aligned} \tag{10}$$

$$[\vec{m}_1(x_1^{(2)})]_{\max} = \max\{\vec{m}_1(x_1^{(2)})\} \to 0.85 \to A_3,$$
$$[\vec{m}_2(x_2^{(2)})]_{\max} = \max\{\vec{m}_2(x_2^{(2)})\} \to 0.8 \to B_4,$$
$$[\vec{m}(y^{(2)})]_{\max} = \max\{\vec{m}(y^{(2)})\} \to 0.6 \to C_4.$$

$$\mu(R_l(2)) = (0.85)(0.8)(0.6) = 0.408. \tag{11}$$

So we choose this rule in place of the above rule so that it will be

$$R_l(1): \text{ IF } (x_1 \text{ is } A_3 \text{ and } x_2 \text{ is } B_4) \text{ THEN } y \text{ is } C_4 \tag{12}$$

Step 4: Refining the Selection of Associated Membership Functions Set Numbers
Calculate the average truth degree of all extracted rules as:

$$\mu_{av} = \sum_{i=1}^{n} \mu(R(i))/n \tag{13}$$

where n is the number of extracted rules.

We change the number of fuzzy sets associated with each input and output variable and repeat the above steps for every possible combination for prescribed numbers of associated fuzzy sets for every variable. The group which gives maximum average μ_{av} is chosen. The learning algorithm with its 4 steps can be summarized as shown in the flow chart of Fig. 21. If we view this four step procedure as a block, then the inputs to this block are examples and the output is the best group of fuzzy rules expressing these examples with their associated membership functions, (Zyada et al, 2006-A).

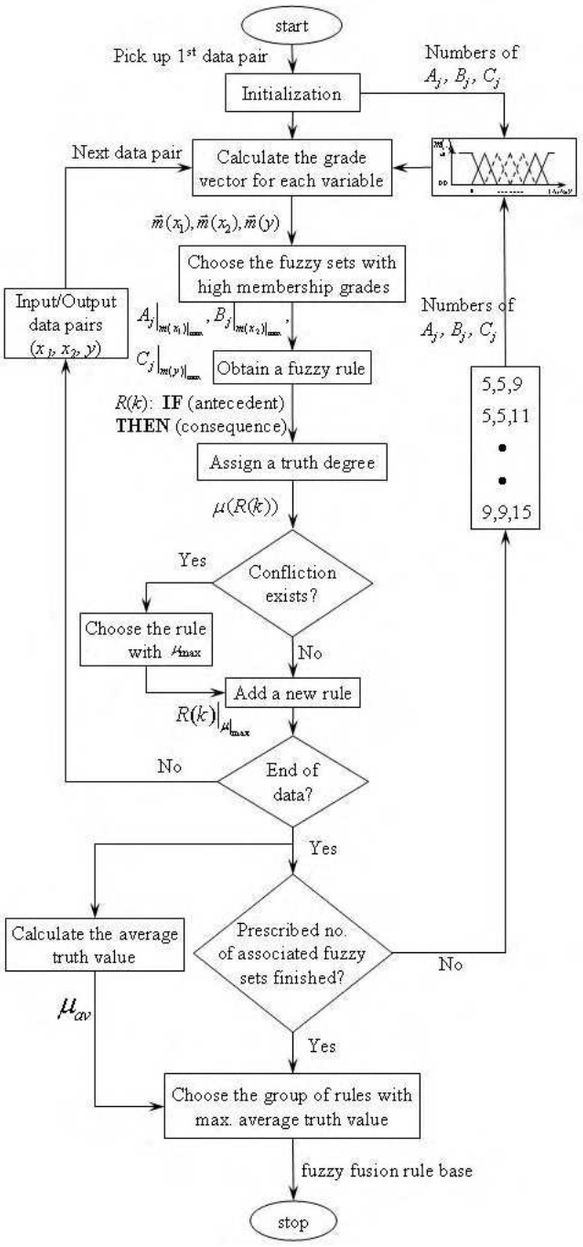

Fig. 21. Learning algorithm flow chart

4.3.2 Learning Fuzzy Rules for GPR-MD Fusion

For the system described in section II, the scanning path is designed as shown in Fig. 15. The manipulator scanned the object, dummy PMN2 landmine, while it is buried at different depths. The depth is changed from 0.0 to 70.0 mm in steps of 10 mm. The depth is measured from the ground surface to the upper face of the dummy land mine. The depth is limited to the maximum depth at which a land mine could be sensed by a metal detector, (70 mm in our case). The gap between the sensor head, (both GPR and MD), and the ground surface is kept constant at 10 mm during all experiments. The sensors positioning variables are treated as crisp not as fuzzy variables in the current work. The data is acquired for both GPR and MD scanning. The signal for both sensors is processed as described in section III. The output of processing is the values of GPR and MD features at different depths. These values are input to the learning algorithm described in the first part of this section, as shown in Fig. 22.

	IF Part		THEN Part
No.	MD Feature	GPR Feature	
1	A1	B1	C7
2	A3	B3	C6
3	A3	B4	C5
4	A5	B6	C4
5	A2	B7	C3
6	A1	B8	C2
7	A3	B9	C1

Table 1. Learnt fuzzy fusion rules

The output is a group of fuzzy rules that best express these GPR and MD features. The output fuzzy rules are shown in Table 1, [18], where A's, B's and C's fuzzy sets are changing from low to high, (i.e. A1 is smaller than A2, B1 is smaller than B2, C1 is smaller C2, and so on). Because of the limited number of training data, the learnt fuzzy rules are few for association. A solution for this problem is to increase the number of training data through interpolation. We applied linear interpolation for the extracted features and re-applied the learning algorithm of Fig. 22. The result is a better number of fuzzy rules suitable for rules association as shown in Table 2.

MD Variable \ GPR Variable	A1	A2	A3	A4	A5	A6	A7
B1			C9				
B2			C8	C7	C7	C7	
B3			C5	C6	C6	C6	C6
B4	C3	C3	C4				
B5	C2	C1					

Table 2. Learnt fuzzy fusion rules after interpolation

4.4 Experimental Evaluation

The A decision making system, Fig. 23, is proposed for evaluating the learnt fuzzy fusion rules. The inputs of the decision making system are the extracted features for both MD and GPR, the features positions as well as the learnt fuzzy fusion rules. A tested object should fulfill three conditions to be decided as a land mine: 1) position of features of both GPR and MD should be near from each other. MD feature position, (MD_Pos), to be near from GPR feature position, GPR_Pos, is defined as the following crisp expression with a specific offset.

$$MD\_Pos - Offset \le GPR\_Pos \le MD\_Pos + Offset \quad (14)$$

In the decision making algorithm, the offset is chosen to be the land mine radius, 2) the object should be detected a landmine suspect by a GPR. It means that GPR feature should be associated in the learnt fuzzy rule base, 3) the object should be detected as a land mine suspect by MD too. The MD feature should be associated within the fuzzy rule base.
In the following, three experimental tests and their results for evaluating the proposed fuzzy rule-based fusion system are presented.

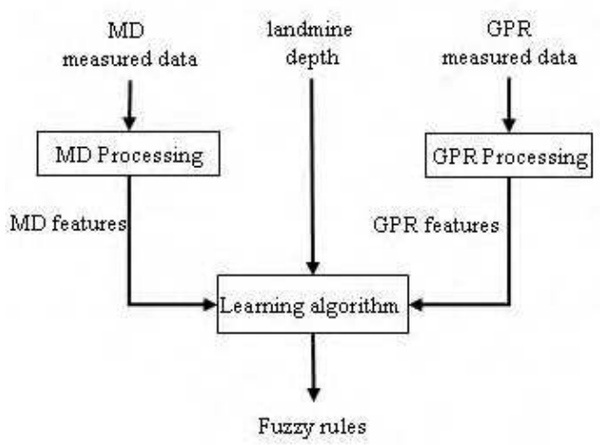

Fig. 22. Fuzzy rules learning algorithm for MD and GPR sensors fusion

4.4.1 Tests

Three tests are carried out with different objects. The first object is the dummy land mine, Fig. 14, at a depth different from that specified in the training phase. The second object is a plastic case, Fig. 8, having the same shape of a land mine in which a metal object, (bolt), is inserted. The third object is a metal bolt only. The three objects can be sensed by both metal detector and ground penetrating radar. Each object is scanned by both MD and GPR. Data is processed and the features as well as their positions are obtained. The features, their positions, learnt fusion rules for a specific tested object are input to fuzzy decision making system, Fig. 23. The positions of landmine suspect features are checked first. If they were near from each other according to definition of (12), the decision making system proceed for fuzzy fusion. The features are fuzzified with the same membership functions obtained in the learning phase. The fuzzified values are compared with the final learnt fusion rules of Table 2 through an implemented MATLAB program. It is based on input fuzzy sets

association, (Yen, 1999). If there is an association then there is a PMN2 landmine and its depth is the output fuzzy rule. If there is no association for any of the features, it means that the object is not the specified PMN2 landmine.

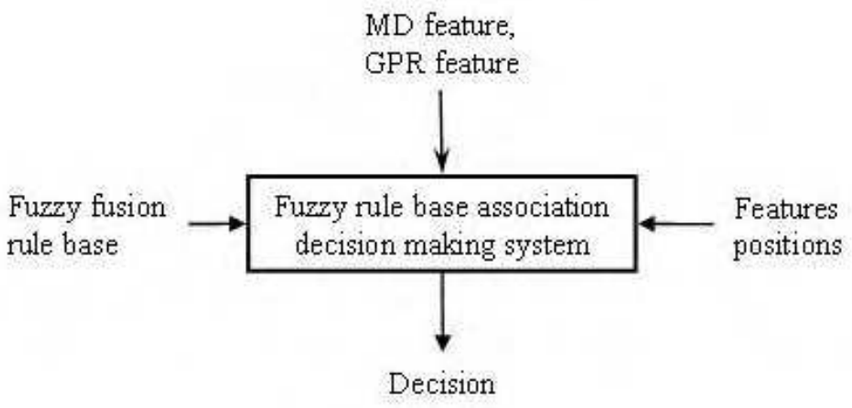

Fig. 23. Decision making system

4.4.2 Performance

The The proposed algorithm could easily classify the first object, (the dummy land mine), and expect its depth to be around 2.3 cm (its surface was actually at a depth of 2.5 cm). The second object, (a case with an inserted metal bolt), as well as the third object, (a metal bolt only), could be classified as a non-land mine object. The second object was detected as a land mine suspect with GPR but not a land mine suspect with MD. There was no association of the MD feature. Also, the third object was not detected as a landmine suspect with either MD or GPR. There was no association of both MD feature and GPR feature. The fulfillment of the decision making conditions as well as the final decision are shown in Table 3, where "O" means the condition is fulfilled and "X" means the condition is not fulfilled.
The decision of the second and third object would be difficult if it to be done by a deminer from GPR images and/or MD sounds (or images). It should be noted here that even though the MD feature of the 2nd object, Table 3, was not fulfilled by the decision making system, MD will give a sound, (or image). Also, even though the GPR feature of the 3rd object, Table 3, was not fulfilled by the decision making system, it will give an image. The features were not fulfilled because their values were outside the range leant during the learning phase. Based on that, the proposed automatic detection algorithm will decrease the false alarm rate significantly. One limitation of the algorithm is that it is based on the association of the input fuzzy rules, (i.e.: if the input fuzzy rules are outside the learnt rules, the algorithm will not give decision). That is the need to modify the decision making to be based on implication in place of association, (Yen, 1999). One more limitation is that the positions of GPR and MD features are treated as crisp variables because a PA10 manipulator, (with its high positioning accuracy), is applied for sensor manipulation. However in a real field, if a mobile vehicle like that presented in section 2, is applied for sensor manipulation, the features' positions are preferably treated as fuzzy variables as well. Fuzzy fusion development will include geography adaptive scanning based fusion in the future.

No.	Object	Features position fulfillment	MD feature fulfillment	GPR feature fulfillment	Decision
1	Dummy land mine	O	O	O	A land mine at an expected depth
2	Plastic case + a metal bolt	O	X	O	Not a land mine
3	A metal bolt	O	X	X	Not a land mine

Table 3. Decision making system results

5. Conclusions

In this chapter, GPR environmental-based landmine automatic detection is presented. The contribution of the presented research can be summarized in: (1) introducing a low-pressure-tire vehicle as a sensor manipulator. It is capable to move inside a mine field without detonating a group of anti-personnel landmines; (2) introducing a signal processing technique for the enhancement of GPR images for an undulating surface. Signal processing for ground adaptive scanning and its image results are presented applying a vector FMCW GPR; (3) an automatic detection method of an anti-personal land mine based on fuzzy fusion rules for GRR-MD is presented. Fuzzy technique is applied for learning a fuzzy rule-base from examples. The proposed method is easy to be implemented in a real field and easy to be executed by a normal operator or a deminer. It was possible to automatically differentiate between a land mine and other objects which would minimize the false alarm rate significantly.

Prospects:

The future work would include: (1) developing the low-pressure-tire vehicle through increasing the contact area between the tire and the ground; (2) extending the presented sensor fusion technique to geography adaptive scanned ground applying both MD and GPR; (3) treating sensors' positions as fuzzy variables in the sensor fusion algorithm.

6. References

Anderson, S. L. (2002). Landmine detection research pushes forward, despite challenges, *IEEE intelligent Systems Magazine*, March/ April 2002, pp. 4-5

Auephanwiriyakul, S., Keller, J. M. and Gader, P. D. (2002). Generalized choquet fuzzy integral fusion, *Information Fusion*, Vol. 3, pp. 69-85.

Branco, P. J. C. and Dente, J. A. (2000). On using Fuzzy Logic to Integrate Learning Mechanisms in an Electro-Hydraulic System-part II: Actuator's Position Control, *IEEE Transactions on Systems, Man, and Cybernetics-Part C: Applications and Reviews*, Vol. 30, No. 3, Aug. 2000, pp. 317-327.

Branco, P. J. C. and Dente, J. A. (2000). On using Fuzzy Logic to Integrate Learning Mechanisms in an Electro-Hydraulic System-part I: Actuator's Fuzzy Modeling,

IEEE Transactions on Systems, Man, and Cybernetics-Part C: Applications and Reviews, Vol. 30, No. 3, Aug. 2000, pp. 305-316.

Branco, P. J. C. and Dente, J.A. (1998). An Experiment in Automatic Modeling an Electrical Drive System using Fuzzy Logic, *IEEE Transactions on Systems, Man, and Cybernetics-Part C: Applications and Reviews*, Vol. 28, No. 2, May 1998, pp. 254-262.

Cremer, F., Schutte, K., Schavemaker, J.G.M. & Breejen, E. den. (2001). A comparison of decision-level sensor-fusion methods for anti-personnel landmine detection, *Information Fusion*, No. 2, 2001, pp. 187-208.

Daniels, D.J. (2004). *Ground Penetrating Radar*, 2nd Edition, The Institution of Electrical Engineers, London, UK, 2004.

Feng, X. and Sato, M. (2004). Pre-stack migration applied to GPR for landmine detection, *Inverse Problems* 20 S99-S1115.

Fukuda, T., Hasegawa, Y., Kawai, Y., Sato, S., Zyada, Z. & Matsuno, T. (2006). Automatic landmine detection system using adaptive sensing with vector GPR, *Proceedings of 32nd Annual Conference of IEEE Industrial Electronics Society*, IECON06, Paris, 7-10 Nov. 2006, pp. 4498-4503.

Fukuda, T., Hasegawa, Y., Kawai, Y., Sato, S., Zyada, Z. & Matsuno, T. (2007). GPR signal processing with geography adaptive scanning using vector radar for anti-personal landmine detection, *International Journal of Advanced Robotic Systems*, Vol. 4, No. 2, 2007, pp. 199-206.

Fukuda, T., Yokoe, K., Hasegawa, Y. and Fukui, T., "Land mine detection algorithm using ultra wide band GPR," *Proceedings of the 1st International Symposium on Systems and Human Science*, 2003, pp. 295-300.

Gader, P.D., Keller, M. & Nelson, B.N. (2001). Recognition technology for the detection of buried land mines, *IEEE transactions on fuzzy systems*, Vol. 9, No. 1, 2001, pp. 31-43.

Genève International Centre for Humanitarian Demining, A Guide to Mine Action, http://www.gichd.ch/96.0.html, pp.63–77

Hasegawa, Y., Kawai, Y., Yokoe, K. & Fukuda, T. (2004)-A. Low-ground-pressure vehicle for adaptive mine detection, *Proceedings of Joint International Conference on Soft Computing and Intelligent Systems and 5th International Symposium on Advanced Intelligent Systems*, 2004, pp. - .

Hasegawa, Y., Kawai, Y., Yokoe, K. & Fukuda, T. (2005). Automatic extraction for mine suspects from GPR, Proceedings of IARP International Workshop on Robotics and Mechanical Assistance in Humanitarian Demining (HUDEM2005), (June 2005), pp. 27-32.

Hasegawa, Y., Yokoe, K., Kawai, Y. & Fukuda, T. (2004)-B. GPR-based adaptive sensing, *Proceedings of 2004 IEEE/RSJ International Conference on Intelligent Robotics and Systems*, (2004), Sendai, Japan, pp. 3021-3026.

Kato, K. and Hirose, S. (2001). Development of the quadruped walking robot, titan-ix - mechanical design concept and application for humanitarian demining robot. In Advanced Robotics, VSP and Robotics Society of Japan, 2001, Vol. 15, pp. 191-204.

Kimura, N. et al. (1992). Development of Radar for Investigation of Buried Objects (First Report), National Convention of the Institute of Electrical Engineers of Japan 1992, (1992), pp.P1 :64–P1 :65

Milisavljevic, N. & Bloch, I.. (2003). Sensor fusion in anti-personnel mine detection using a two-level belief function model, *IEEE Trans. On Systems Man and Cybernetics-Part C*, Vol. 33, No. 2, 2003, pp. 269-283.

Murasawa, K. et al.. (1992). Development of Radar for Investigation of Buried Objects (Second Report), National Convention of the Institute of Electrical Engineers of Japan 1992, ,(1992), pp. P1 :66–P1 :67

Nonami, K. (2002). Development of mine detection robot comet-ii and comet-iii. Proceedings of the 41st SICE Annual Conference (SICE 2002), August 2002, Vol. 1, pp. 5-7.

Sato, M., Fujiwara, J., Feng, X., Zhou, Z. and Kobayashi, T. (2005). Development of a hand-held GPR MD sensor system (ALIS), *Proceedings of SPIE-the International Society for Optical engineering*, Vol. 5794, June 2005, pp. 1000-1007.

Schneider, W. A. (1978). Integral formulation for migration in two and three dimensions, *Geophysics* 43, 1978, pp. 49-76.

Shimoi, N. (2002). Technology for detecting and clearing LANDMINES, Morikita Shuppan Co., Ltd., (2002), pp.43, pp.66–81

Siegel, R. (2002). Land mine detection, *IEEE Instrumentation & Measurement Magazine*, December 2002, pp. 22-28.

Van Dam, R. L., Borchers, B. and Hendrickx, J. M. H. (2005). Strength of landmine signatures under different soil conditions: implications for sensor fusion, *International Journal of Systems Science*, Vol. 36(9), 2005, pp. 573-588.

Wang, L. X. and Mendel, J. (1992). Generating fuzzy rules by learning from examples, *IEEE Trans. Syst., Man, Cybern.*, Vol. 24, Feb. 1992, pp. 332-342.

Yen, J. (1987). Fuzzy logic-a modern perspective, *IEEE transactions on knowledge and data engineering*, Vol. 11, No. 1, (January/February 1999), pp. 153-165.

Yilmaz, O. (1987). *Seismic Data Processing*, (Tulsa, Oklahoma: Society of Exploration Geophysics).

Zadeh, L. A. (1973). Outline of a New Approach to the Analysis of Complex Systems and Decision Processes, *IEEE Transactions on Systems, Man, and Cybernetics*, Vol. SMC-3, No. 1, January 1973, pp. 28-44.

Zyada, Z., Hasegawa, Y. and Fukuda, T. (2002). Implementing Fuzzy Learning Algorithms in a 6 DOF Hydraulic Parallel Link Manipulator: Control with Actuators' Forces Fuzzy Compensation, *Journal of Advanced Computational Intelligence*, JACI, Vol.6 No.3, 2002, pp. 100-108.

Zyada, Z., Hasegawa, Y., Vachkov, G. and Fukuda, T. (2002). Implementing fuzzy learning algorithms in a 6 DOF hydraulic parallel link manipulator: actuators' fuzzy modelling, *Journal of Robotics and Mechatronics*, Vol. 14, No. 4, 2002, pp.408-419.

Zyada, Z., Kawai, Y., Matsuno, T. & Fukuda, T. (2006)-A. Fuzzy sensor fusion for mine detection, *Joint 3rd International Conference on Soft Computing and Intelligent Systems, 7th International Symposium on Advanced Intelligent Systems*, SCIS-ISIS 2006, Tokyo, (September 2006), pp. 349-354.

Zyada, Z., Kawai, Y., Matsuno, T. & Fukuda, T. (2006)-B. Sensor fusion based fuzzy rules learning for humanitarian mine detection, *SICE-ICASE International Joint Conference 2006*, Bussan, Korea, (October 2006).

Zyada, Z., Kawai, Y., Matsuno, T. & Fukuda, T. (2007). Fuzzy sensor fusion for humanitarian demining, *Journal of Advanced Computational Intelligence and Intelligent Informatics*, *To appear in* Vol. 11, No. 7, 2007.

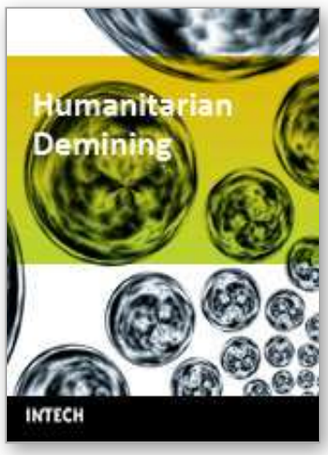

Humanitarian Demining

Edited by Maki K. Habib

ISBN 978-3-902613-11-0
Hard cover, 392 pages
Publisher I-Tech Education and Publishing
Published online 01, February, 2008
Published in print edition February, 2008

United Nation Department of Human Affairs (UNDHA) assesses that there are more than 100 million mines that are scattered across the world and pose significant hazards in more than 68 countries. The international Committee of the Red Cross (ICRC) estimates that the casualty rate from landmines currently exceeds 26,000 persons every year. It is estimated that more than 800 persons are killed and 1,200 maimed each month by landmines around the world. Humanitarian demining demands that all the landmines (especially AP mines) and ERW affecting the places where ordinary people live must be cleared, and their safety in areas that have been cleared must be guaranteed. Innovative solutions and technologies are required and hence this book is coming out to address and deal with the problems, difficulties, priorities, development of sensing and demining technologies and the technological and research challenges. This book reports on the state of the art research and development findings and results. The content of the book has been structured into three technical research sections with total of 16 chapters written by well recognized researchers in the field worldwide. The main topics of these three technical research sections are: Humanitarian Demining: the Technology and the Research Challenges (Chapters 1 and 2), Sensors and Detection Techniques for Humanitarian Demining (Chapters 3 to 8), and Robotics and Flexible Mechanisms for Humanitarian Demining respectively (Chapters 9 to 16).

INTECH
open science | open minds

InTech Europe
University Campus STeP Ri
Slavka Krautzeka 83/A
51000 Rijeka, Croatia
Phone: +385 (51) 770 447

InTech China
Unit 405, Office Block, Hotel Equatorial Shanghai
No.65, Yan An Road (West), Shanghai, 200040, China
中国上海市延安西路65号上海国际贵都大饭店办公楼405单元
Phone: +86-21-62489820

Fax: +385 (51) 686 166
www.intechopen.com

Fax: +86-21-62489821

IntechOpen